AUT Journal of Modeling and Simulation

AUT J. Model. Simul., 54(2) (2022) 161-172
DOI: 10.22060/miscj.2022.21580.5290

Tilt estimation using pressure sensors for unmanned underwater vehicle navigation

M. Amuei[1], S. M. Dehghan[1]*, H. Nourmohammadi[2], M. AlirezaPouri[1]

[1] Faculty of Electrical and Computer Engineering, Malek-Ashtar University of technology, Tehran, Iran
[2] Northern Research Center for Science and Technology, Malek-Ashtar University of technology, Fereydunkenar, Iran

ABSTRACT: Since the Unmanned Underwater Vehicles (UUVs) don't receive the Global Navigation Satellite System (GNSS) signals under the water, other aided measurements are needed to provide the required accuracy in tilt estimation including roll and pitch angle estimation. Conventional approaches for pressure-based tilt estimation, only consider the relation between the static pressure and the tilt as the measurement model. However, the performance of this approach depends on the dynamic pressure which is caused by the sea waves. This paper improves the accuracy of pressure-based tilt estimation using the more accurate of the measurement model. Also, the proposed approach considers the coupling between the axes of UUV. Due to the cost of the approach and the hardware limitations of installation pressure sensors, the proposed approach is implemented using two pressure sensors. An Extended Kalman Filter (EKF) is used for simultaneous tilt and gyroscopes measurement errors estimation. A Monte-Carlo simulation is developed to evaluate the performance of the proposed approach in comparison with INS only and the conventional static pressure-based tilt estimation. The simulation results show that tilt estimation performance of conventional approach is better than the INS only performance and the performance of proposed approach is better than the both of them.

Review History:

Received: Jul. 10, 2022
Revised: Dec. 04, 2022
Accepted: Dec. 19, 2022
Available Online: Feb. 28, 2023

Keywords:

Pressure sensor
static and dynamic pressure
tilt estimation
Extended Kalman filter
unmanned underwater vehicle.

1- Introduction

INS is one of the main systems for UUV navigation. Due to incremental orientation error of INS, auxiliary sensors are used to reduce orientation error [1]. Using GNSS and Doppler Velocity Logger (DVL) are common approaches to decrease this error. But, DVL has dimensional and technological limitations and GNSS signals aren't received under water. Also, there are some approaches to improve yaw angle estimation such as using magnetometer [2], but these approaches cannot be used for tilt estimation improvement. Using pressure sensors is one of the suitable methods for this purpose.

There are some researches which use pressure sensors to measure orientation. In [3] a method for attitude estimation is proposed which utilizes the depth and velocity measurement. Then orientation is calculated using pressure and velocity measurement. Needing velocity measurements is the problem with this method which should be measured with velocity instruments such as DVL. In [4], tilt is estimated using a group of pressure sensors and minimum least square error method. In this research the estimation of tilt is improved by optimization of pressure sensors configuration based on Cramer-Rao lower bound. In [5], four pressure sensors have been placed on a cross-section of Autonomous Underwater Vehicle (AUV). The relationship between the measurements of pressure sensors and tilt has been established, based on the theoretical analysis. In this research, a multi-sensor integrated system of AUV combined with tri-axial gyroscope, magnetic compass and pressure sensor array has been designed. In [4] and [5], only static pressure has been considered and this causes inaccuracy when the dynamic of environment increases. In [6], an Artificial Lateral Line Sensor (ALLS) system based on a pressure sensor array is proposed to perform pitch motion perception for AUVs. The proposed ALLS system has been fabricated in the fish robot. Then sensing experiments in the conditions of different pitch motions of the robot is conducted and the experimental measurements are compared with numerical simulation results. This research uses a lot of pressure sensors to perform pitch motion perception and the cost and the complexity of the method is increased. More important, this method just performs pitch motion perception and tilt can't be estimated. In [7], the uncertainty study of a pressure sensor underwater system MEMS is addressed and is showed which the accuracy of inertial system relates to the distance of pressure sensors. Research [7] has distance limitation in arranging pressure sensors and the configuration is depended on hardware of the platform. Also, simultaneous rotations around different axis of UUV have been neglected in this research.

All the cited researches focused on static pressure and they have installation limitations and neglecting the simultaneous rotations around different axis. Also, there are a few works in

*Corresponding author's email: SMMD@mut.ac.ir

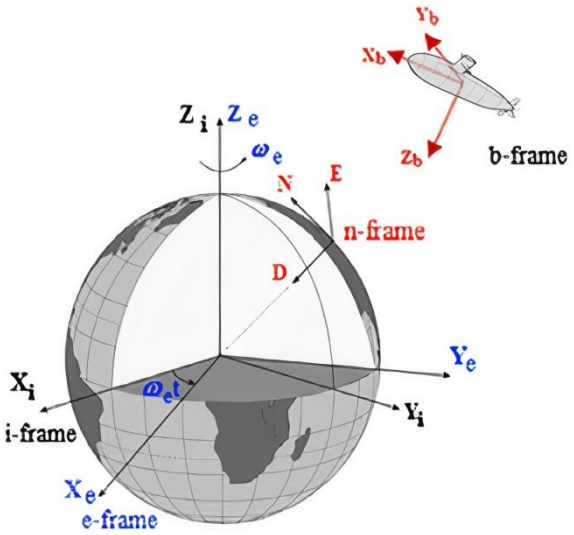

Fig. 1. Reference frames in the inertial navigation

this field, so this can be an appropriate field for researching. In this research, static pressure, and the dynamic of sea waves are taken into account. These increase the accuracy of approach in high dynamic environments. Also, the proposed approach just uses two pressure sensors due to installation limitations and the cost of method. In other words, this paper wants to solve tilt accurate estimation problem without using auxiliary sensors such DVL and GNSS. The proposed approach can be used to estimate tilt of UUVs in many applications. We test the proposed method in an UUV navigation simulation loop which estimates gyroscope bias and orientation and explain this loop in detail in section 6.

The main contributions of the paper can be summarized as follows:

Improvement of UUV navigation with pressure sensors

Increase accuracy of the UUV navigation by considering dynamic pressure in tilt estimation

Propose a low-cost method using two pressure sensors

The rest of this paper is organized as follows. Section 2 describes the problem statement of paper. Section 3 and 4 describes the system model and measurement model, respectively. Section 5 stands for the state estimation filter and explain the tilt estimation using the pressure sensors. Simulation results investigate in section 6 and section 7 concludes the paper.

2- Problem Statement

In this section the concepts of tilt estimation using pressure sensors is described. First, we introduce the reference frames used in the text including inertial frame (i-frame), earth frame (e-frame), navigation frame (n-frame) and body frame (b-frame) as illustrated in Fig. 1 [8].

The purpose is estimation of tilt in the lake of technological limitations of accurate speed sensors and GNSS signals under water. So, we need to estimate tilt by pressure sensors. The pressure sensors dispose the static and dynamic pressure of water. But, the conventional approaches only consider the relation between the static pressure and the tilt as the measurement model and this causes inaccuracy in tilt estimation. Also, due to cost limitations and installation limitations of pressure sensors in an UUV, the proposed approach just use two pressure sensors. The accuracy of sensors installation place affects on the accuracy of tilt estimation. Then, the best place for sensors installation is under the UUV. Increasing the distance of the pressure sensors improves the accuracy estimation of tilt. Also, due to the effect of hydrodynamic disturbance in measurements, the two sensors should be installed away from nose and tail on a flat place of the UUV. Considering these explanations, the sensors have been installed in the bottom of UUV in the direction of longitudinal-axis as shown in Fig. 2.

In Fig. 2, The origin of the body frame (point) is located on the center of UUV. and are the position of the sensors 1 and 2 in the body frame, respectively. In the proposed approach, total measured pressure has a nonlinear relationship with tilt. So, EKF is an appropriate estimator for tilt estimation. The block diagram of proposed approach is illustrated in Fig. 3.

As shown in Fig. 3, total pressure is measured by pressure sensors and these measurements are used in EKF for tilt estimation. Estimated tilt can be used for UUV navigation to increase the accuracy of the navigation. In sections 3 to 5 we explain the implementation for tilt estimation.

3- System Dynamic

System dynamic includes tilt dynamic model. Therefore, the state vector is constituted by tilt as follows:

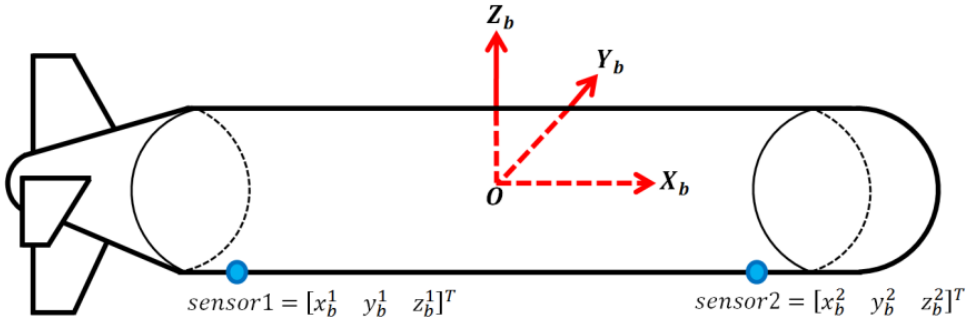

Fig. 2. Installation place of two sensors in UUV

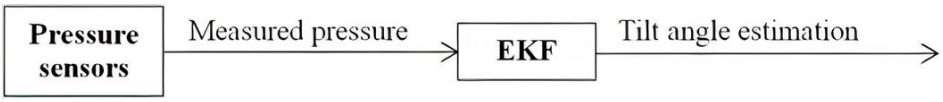

Fig. 3. Block diagram of proposed approach

$$\boldsymbol{X}_P = \begin{bmatrix} \phi_P & \theta_P \end{bmatrix}^T \tag{1}$$

Where, ϕ_P and θ_P stands for roll and pitch angle, respectively. Dynamic model of roll angle describes as (2) [9]:

$$\dot{\phi}_P = p + q \sin\phi_P \tan\theta_P + r \cos\phi_P \tan\theta_P \tag{2}$$

In (2), $\begin{bmatrix} p & q & r \end{bmatrix}^T$ is the output of UUV gyroscope in body frame. Also, pitch angle dynamic model is as follows [9]:

$$\dot{\theta}_P = q \cos\phi_P - r \sin\phi_P \tag{3}$$

So, the dynamic of system is defined as:

$$\dot{\boldsymbol{X}}_P = g\left(\boldsymbol{X}_P, \boldsymbol{u}\right) + \boldsymbol{W}_P \quad , \quad \boldsymbol{W}_P \sim N\left(0, \boldsymbol{Q}_P\right) \tag{4}$$

Where, $\boldsymbol{Q}_P$ is the covariance matrix of the system dynamic and considering (2) and (3), $g\left(\boldsymbol{X}_P, \boldsymbol{u}\right)$ and can be defined as:

$$g\left(\boldsymbol{X}_P, \boldsymbol{u}\right) = \begin{bmatrix} p + q \sin\phi_P \tan\theta_P + r \cos\phi_P \tan\theta_P \\ q \cos\phi_P - r \sin\phi_P \end{bmatrix} , \quad \boldsymbol{u} = \begin{bmatrix} p & q & r \end{bmatrix}^T \tag{5}$$

4- Measurement System

This section describes measurement system including pressure sensors measurement. So, the measurement vector is constituted as:

$$\boldsymbol{Z}_P = \begin{bmatrix} P_{sensor_1} & P_{sensor_2} \end{bmatrix}^T \tag{6}$$

Where, P_{sensor_1} and P_{sensor_2} are the measured pressure by sensor 1 and 2, respectively. As mentioned in section 1, static and dynamic pressures have been considered together. Therefore, pressure sensor measurement can be model as follows:

$$P_{sensor} = P_0 + P_{static} + P_{dynamic} \tag{7}$$

In (7), P_0 is sea level pressure and is almost equal to Pascale, P_{static} is the static pressure due to the depth of sensor

and $P_{dynamic}$ is the dynamic pressure due to the effect of sea wave dynamic. P_{static} can be modeled as follows [10]:

$$P_{static} = \rho g d \tag{8}$$

Where, ρ, g and d are the density of sea water, gravity acceleration and depth of UUV, respectively. Also, the dynamic pressure describes as [11]:

$$P_{dynamic} = A\rho g e^{-kd}\cos\left(kx-\omega t\right) \tag{9}$$

Where, A is the altitude of sea waves, k is the numbers of sea wave in length of x, ω is the angular frequency and t is time. Eq. (9) can be summarized as (10) due to the less effect of sinusoidal term [11]:

$$P_{dynamic} = A\rho g e^{-kd} \tag{10}$$

So, the measurement system is defined as follows:

$$\boldsymbol{Z}_P = h\left(\boldsymbol{X}_P\right)+\boldsymbol{V}_P \quad , \quad \boldsymbol{V}_P \sim N\left(0,\boldsymbol{R}_P\right) \tag{11}$$

$\boldsymbol{R}_P$ is the measurement covariance matrix and $h\left(\boldsymbol{X}_P\right)$ can be defined with expanding (7). Eq. (8) and (10) can be considered for expanding (7) as:

$$P_{sensor} = P_0 + \rho g d + A\rho g e^{-kd} \tag{12}$$

Also, the origin position of body frame is zero, e.g. $\begin{bmatrix} x_b^o & y_b^o & z_b^o \end{bmatrix}^T = \begin{bmatrix} 0 & 0 & 0 \end{bmatrix}^T$, then we obtain [4]:

$$\begin{bmatrix} x_n^i \\ y_n^i \\ z_n^i \end{bmatrix} - \begin{bmatrix} x_n^o \\ y_n^o \\ z_n^o \end{bmatrix} = C_b^n \begin{bmatrix} x_b^i \\ y_b^i \\ z_b^i \end{bmatrix} \quad ,$$
$$C_b^n = \begin{bmatrix} c\theta_P c\psi_P & s\phi_P s\theta_P c\psi_P - c\phi_P s\psi_P & c\phi_P s\theta_P c\psi_P + s\phi_P s\psi_P \\ c\theta_P s\psi_P & s\phi_P s\theta_P c\psi_P + c\phi_P c\psi_P & c\phi_P s\theta_P c\psi_P - s\phi_P c\psi_P \\ -s\theta_P & s\phi_P c\theta_P & c\phi_P c\theta_P \end{bmatrix} \tag{13}$$

Where, $\begin{bmatrix} x_n^i & y_n^i & z_n^i \end{bmatrix}^T$ and $\begin{bmatrix} x_n^o & y_n^o & z_n^o \end{bmatrix}^T$ stand for the position vector of i[th] sensor and the position vector of body frame origin in navigation frame, respectively. Also, $\begin{bmatrix} x_b^i & y_b^i & z_b^i \end{bmatrix}^T$ is the position vector of i[th] sensor in body frame. Then, the third element of (13) becomes as:

$$z_n^i - z_n^o = -x_b^i\left(s\theta_P\right) + y_b^i\left(s\phi_P c\theta_P\right) + z_b^i\left(c\phi_P c\theta_P\right) \tag{14}$$

Consequently, the depth of i[th] sensor can be calculated by (14) as:

$$d = -x_b^i\left(s\theta_P\right) + y_b^i\left(s\phi_P c\theta_P\right) + z_b^i\left(c\phi_P c\theta_P\right) + z_n^o \tag{15}$$

Considering (12) and (15), P_{sensor} for the i[th] sensor is as (16):

$$\begin{aligned} P_{sensor_i} &= P_0 + \rho g\left(-x_b^i\left(s\theta_P\right) + \right. \\ &\quad \left. y_b^i\left(s\phi_P c\theta_P\right) + z_b^i\left(c\phi_P c\theta_P\right) + z_n^o\right) \\ &\quad + A\rho g e^{-k\left(-x_b^i\left(s\theta_P\right)+y_b^i\left(s\phi_P c\theta_P\right)+z_b^i\left(c\phi_P c\theta_P\right)+z_n^o\right)} \end{aligned} \tag{16}$$

Accordingly, $h\left(\boldsymbol{X}_P\right)$ can be defined as:

$$h\left(\boldsymbol{X}_P\right) = \begin{bmatrix} P_0 + \rho g\left(-x_b^1\left(s\theta_P\right) + y_b^1\left(s\phi_P c\theta_P\right) + \right. \\ P_0 + \rho g\left(-x_b^2\left(s\theta_P\right) + y_b^2\left(s\phi_P c\theta_P\right) + \end{bmatrix} \tag{17}$$
$$\begin{bmatrix} \left. z_b^1\left(c\phi_P c\theta_P\right) + z_n^o\right) + A\rho g e^{-k\left(-x_b^1\left(s\theta_P\right)+y_b^1\left(s\phi_P c\theta_P\right)+z_b^1\left(c\phi_P c\theta_P\right)+z_n^o\right)} \\ \left. z_b^2\left(c\phi_P c\theta_P\right) + z_n^o\right) + A\rho g e^{-k\left(-x_b^2\left(s\theta_P\right)+y_b^2\left(s\phi_P c\theta_P\right)+z_b^2\left(c\phi_P c\theta_P\right)+z_n^o\right)} \end{bmatrix}$$

5- State Estimation Filter

Due to nonlinearity of tilt dynamic model and measurement system, EKF applied as state estimation filter. Then, the EKF formulation is defined in two steps as prediction and correction phase [12].

Prediction phase:

Predicted state estimate

$$\hat{\boldsymbol{X}}_{k|k-1} = g\left(\hat{\boldsymbol{X}}_{k-1|k-1}, \boldsymbol{u}_k\right)$$

Predicted covariance estimate

$$\mathbf{P}_{k|k-1} = \mathbf{G}_k \mathbf{P}_{k-1|k-1} \mathbf{G}_k^{\,T} + \mathbf{Q}_k$$

Correction phase:

Innovation or measurement residual

$$\tilde{\mathbf{y}}_k = \mathbf{Z}_k - h\left(\hat{\mathbf{X}}_{k|k-1}\right)$$

Innovation (or residual) covariance

$$\mathbf{S}_k = \mathbf{H}_k \mathbf{P}_{k|k-1} \mathbf{H}_k^{\,T} + \mathbf{R}_k \tag{18}$$

Kalman gain

$$\mathbf{K}_k = \mathbf{P}_{k|k-1} \mathbf{H}_k^{\,T} \mathbf{S}_k^{\,-1}$$

Update state estimate

$$\hat{\mathbf{X}}_{k|k} = \hat{\mathbf{X}}_{k|k-1} + \mathbf{K}_k \tilde{\mathbf{y}}_k$$

Update covariance estimate

$$\mathbf{P}_{k|k} = \left(\mathbf{I} - \mathbf{K}_k \mathbf{H}_k\right) \mathbf{P}_{k|k-1}$$

Where $\boldsymbol{G}$ and $\boldsymbol{H}$ matrices for EKF can be calculated as follows:

$$\mathbf{G}_k = \left.\frac{\partial g\left(\boldsymbol{X}_P, \boldsymbol{u}\right)}{\partial \mathbf{X}}\right|_{\hat{\mathbf{X}}_{k-1|k-1}} \quad , \quad \mathbf{H}_k = \left.\frac{\partial h\left(\boldsymbol{X}_P\right)}{\partial \mathbf{X}}\right|_{\hat{\mathbf{X}}_{k|k-1}} \tag{19}$$

In (19), k index is the time. Consequently, $\boldsymbol{G}$ and $\boldsymbol{H}$ matrices are as follows:

$$\mathbf{G}_k = \begin{bmatrix} \left(q\cos\phi_P - r\sin\phi_P\right)\tan\theta_P & \left(q\sin\phi_P + r\cos\phi_P\right)\left(1+\tan^2\left(\theta_P\right)\right) \\ -q\sin\phi_P - r\cos\phi_P & 0 \end{bmatrix} \tag{20}$$

$$\mathbf{H}_k = \begin{bmatrix} \mathrm{h}_{11} & \mathrm{h}_{12} \\ \mathrm{h}_{21} & \mathrm{h}_{22} \end{bmatrix}$$

Where:

$$\mathrm{h}_{11} = \rho.g.\left(\begin{array}{l}\left(\mathrm{y}_\mathrm{b}^1\cos\hat{\phi}_P.\cos\hat{\theta}_P - \mathrm{z}_\mathrm{b}^1\sin\hat{\phi}_P.\cos\hat{\theta}_P\right)\times \\ \left(A.k.e^{-k\left(\mathrm{x}_\mathrm{b}^1\sin\left(\hat{\theta}_P\right)-\mathrm{y}_\mathrm{b}^1\sin\left(\hat{\phi}_P\right)\cos\left(\hat{\theta}_P\right)-\mathrm{z}_\mathrm{b}^1\cos\left(\hat{\phi}_P\right)\cos\left(\hat{\theta}_P\right)\right)}-1\right)\end{array}\right)$$

$$\mathrm{h}_{12} = \rho.g.\left(\begin{array}{l}\left(\mathrm{x}_\mathrm{b}^1\cos\hat{\theta}_P + \mathrm{y}_\mathrm{b}^1\sin\hat{\phi}_P.\sin\hat{\theta}_P + \mathrm{z}_\mathrm{b}^1\cos\hat{\phi}_P.\sin\hat{\theta}_P\right)\times \\ \left(1-A.k.e^{-k\left(\mathrm{x}_\mathrm{b}^1\sin\left(\hat{\theta}_P\right)-\mathrm{y}_\mathrm{b}^1\sin\left(\hat{\phi}_P\right)\cos\left(\hat{\theta}_P\right)-\mathrm{z}_\mathrm{b}^1\cos\left(\hat{\phi}_P\right)\cos\left(\hat{\theta}_P\right)\right)}\right)\end{array}\right)$$

$$\mathrm{h}_{21} = \rho.g.\left(\begin{array}{l}\left(\mathrm{y}_\mathrm{b}^2\cos\hat{\phi}_P.\cos\hat{\theta}_P - \mathrm{z}_\mathrm{b}^2\sin\hat{\phi}_P.\cos\hat{\theta}_P\right)\times \\ \left(A.k.e^{-k\left(\mathrm{x}_\mathrm{b}^2\sin\left(\hat{\theta}_P\right)-\mathrm{y}_\mathrm{b}^2\sin\left(\hat{\phi}_P\right)\cos\left(\hat{\theta}_P\right)-\mathrm{z}_\mathrm{b}^2\cos\left(\hat{\phi}_P\right)\cos\left(\hat{\theta}_P\right)\right)}-1\right)\end{array}\right)$$

$$\mathrm{h}_{22} = \rho.g.\left(\begin{array}{l}\left(\mathrm{x}_\mathrm{b}^2\cos\hat{\theta}_P + \mathrm{y}_\mathrm{b}^2\sin\hat{\phi}_P.\sin\hat{\theta}_P + \mathrm{z}_\mathrm{b}^2\cos\hat{\phi}_P.\sin\hat{\theta}_P\right)\times \\ \left(1-A.k.e^{-k\left(\mathrm{x}_\mathrm{b}^2\sin\left(\hat{\theta}_P\right)-\mathrm{y}_\mathrm{b}^2\sin\left(\hat{\phi}_P\right)\cos\left(\hat{\theta}_P\right)-\mathrm{z}_\mathrm{b}^2\cos\left(\hat{\phi}_P\right)\cos\left(\hat{\theta}_P\right)\right)}\right)\end{array}\right)$$

In (20), ϕ_P, θ_P, $\hat{\phi}_P$ and $\hat{\theta}_P$ stand for the last estimated roll, estimated pitch, predicted roll and predicted pitch angle, respectively.

6- Simulation Results

As mentioned in section 1, the proposed approach is tested in an UUV navigation simulation loop illustrated in Fig. 4.

As shown in Fig. 4, the true angular velocity and acceleration in body frame are used for gyroscope and acceleration sensor model and generating reference data. Velocity and position measurement which use in integration with Kalman Filter, have been generated by difference of GNSS and INS position and velocity. Estimated tilt from pressure sensor and measured yaw angle from magnetometer are the other measurements which are used in integration with Kalman Filter. The Estimated gyroscope bias is used to correct angular velocity measurement. Also, the estimated position error and velocity error are used to correct INS position and INS velocity, respectively. As mentioned in section 1, the GNSS signals aren't received under water. So, UUV needs to come up for estimation of position error and velocity error. But, we can estimate orientation and gyroscope bias using pressure sensors and magnetometer all the time.

We use quaternion method [13] in the implementation of UUV navigation by KF. In the simulation, the estimation result using proposed approach has been compared with conventional approach in paper [4] and [5] (which only considers static pressure in measurement model) and INS-only estimation. The evaluation of the proposed and conventional approach has been done based on the block diagram of Fig. 4. In this block diagram, the integration of roll and pitch estimation result and INS output has been demonstrated. It is expected both of conventional and proposed approach can prevent roll and pitch error increasing respect to INS-only and including dynamic pressure in proposed approach can improve the result. In the simulation, the position values of sensor 1 and

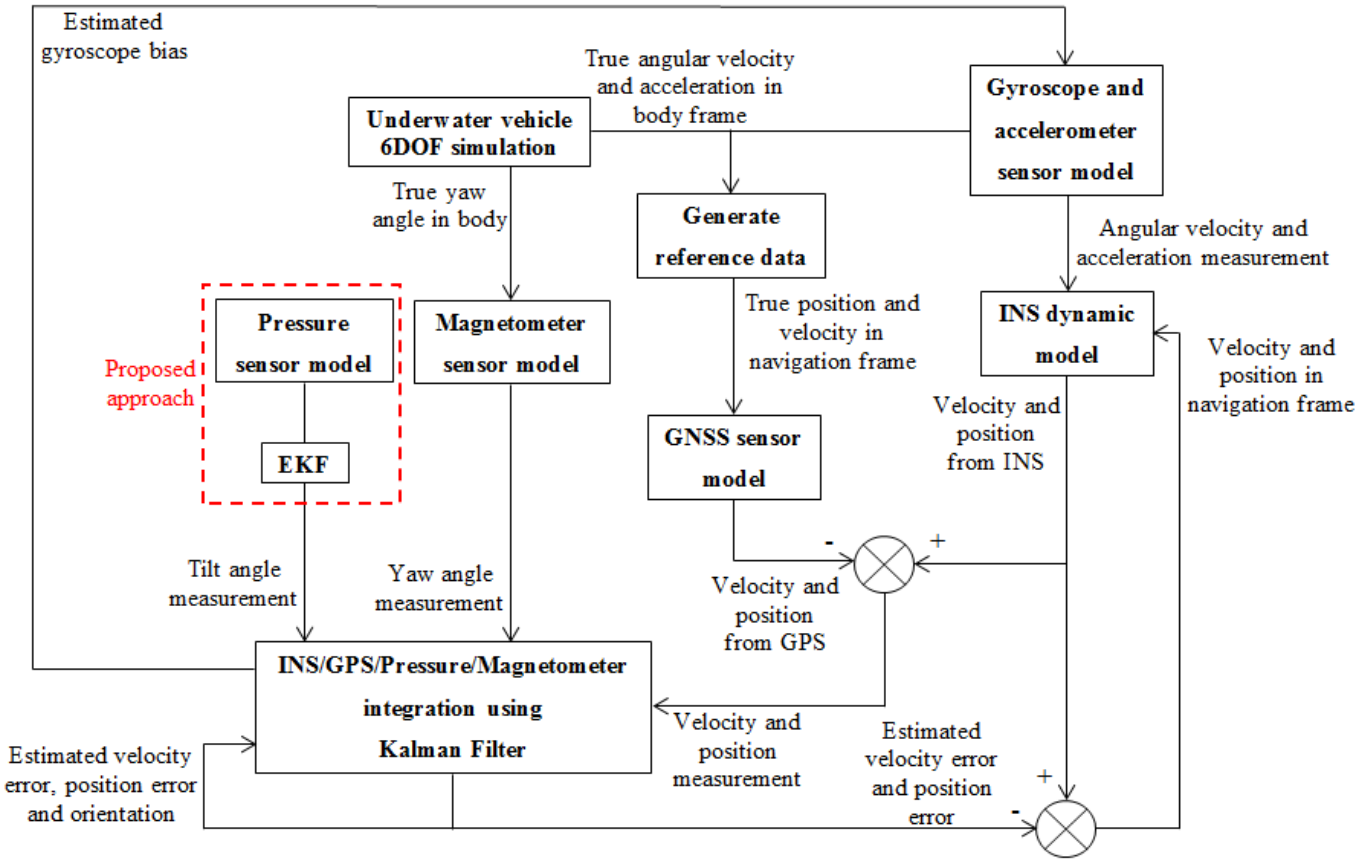

Fig. 4. UUV navigation simulation loop

2 are $\left[x_b^1 \quad y_b^1 \quad z_b^1\right]^T = \left[-1.4 \quad 0 \quad -0.25\right]^T$ (meter) and $\left[x_b^2 \quad y_b^2 \quad z_b^2\right] = \left[1.4 \quad 0 \quad -0.25\right]^T$ (meter), respectively and $A = 1$ (meter), $\rho = 1000\left(\text{kg}/\text{m}^3\right)$, $k = 1$ (1/meter) and $g = 9.8\left(\text{meter}/\text{s}^2\right)$. Also, $\boldsymbol{Q}_{nav} = 0.1\times\boldsymbol{I}_{13\times13}$, $\boldsymbol{R}_{nav} = 0.1\times\boldsymbol{I}_{10\times10}$ (used in UUV navigation), $\boldsymbol{Q}_P = 0.1\times\boldsymbol{I}_{2\times2}$, $\boldsymbol{R}_P = 0.1\times\boldsymbol{I}_{2\times2}$ (used in tilt estimation) and the diameter of UUV is 0.5 (meter). Furthermore, the estimation initial values of state vectors and the estimation covariance matrices considered as $\boldsymbol{X}_{nav} = \left[\left[1 \quad 0 \quad 0 \quad 0\right] \quad 2\times\boldsymbol{I}_{1\times3}\left(\text{meter}\right) \quad \left[10^\circ \quad 10^\circ \quad 1\left(\text{meter}\right)\right] \quad \boldsymbol{0}_{1\times3}\left(\text{deg}/\text{s}\right)\right]^T$, $\mathbf{P}_{nav} = 0.1\times\boldsymbol{I}_{13\times13}$ and $\boldsymbol{X}_P = \boldsymbol{0}_{2\times1}$, $\mathbf{P}_P = 0.1\times\boldsymbol{I}_{2\times2}$ for UUV navigation (using KF) and tilt estimation (using EKF), respectively. The model values of gyroscope bias are considered 0.05, 0.03 and 0.04 (deg/s) along x-axis, y-axis and z-axis, respectively. The trajectory simulation of UUV is shown in Fig. 5 for 10 seconds. The red point in Fig. 5 is the start point of trajectory. The depth changes of trajectory have been considered from -4 to -2.5 meter due to variety of pressure measurement.

Simulation results of UUV tilt and yaw angle estimation are illustrated in Fig. 6 to Fig. 8. It can be seen from Fig. 6 which the measured roll angle by INS only (the red line) are diverged from the model values and finally has 40 degree errors. Although, the estimation roll angle using conventional static pressure (the green line) cannot track the model values and has 3 degree errors from the model values at the end of simulation. The estimated roll angle using proposed approach (the blue line) can track the model values. Similarly, Fig. 6 shows which the measured pitch angle by INS is diverged from the model values and has 20 degree errors after 10 seconds. The estimated pitch angle using conventional approach is diverged from the model values and almost has 1 degree error after 10 seconds. The estimated pitch angle by proposed approach can track the model values, correctly. As referred, the yaw angle has been estimated using magnetometer measurement. Considering Fig. 8 the yaw angle measured by the INS has almost 30 degree errors at the end of simulation, but the estimated values are converged to the model values. Therefore, the simulation results of orientation estimation are satisfied.

Due to using quaternion method in UUV navigation [14], the three times of standard deviation (3σ) and the quaternions estimation error (q_1 to q_4) are illustrated in Fig. 9. All of the estimation errors and 3σ bounds are converged. So, the performance of proposed approach is satisfying.

Simulation results of the UUV gyroscope bias around x,

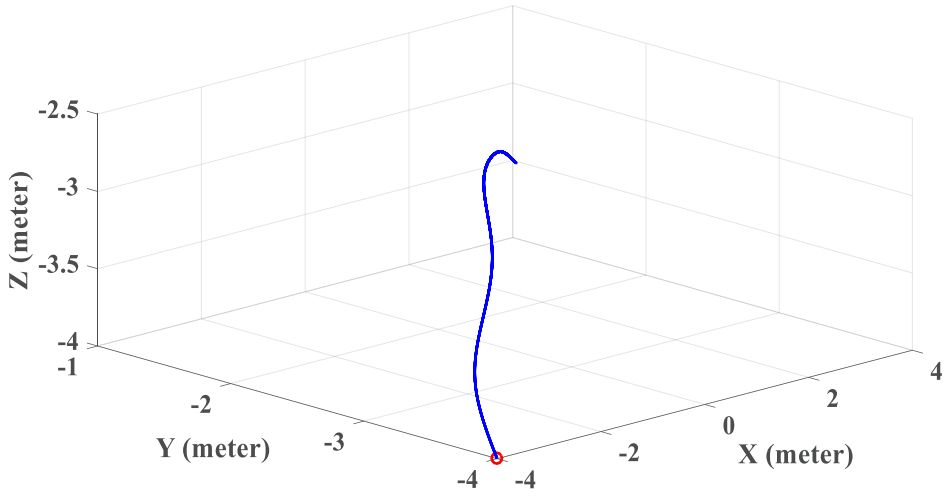

Fig. 5. UUV trajectory

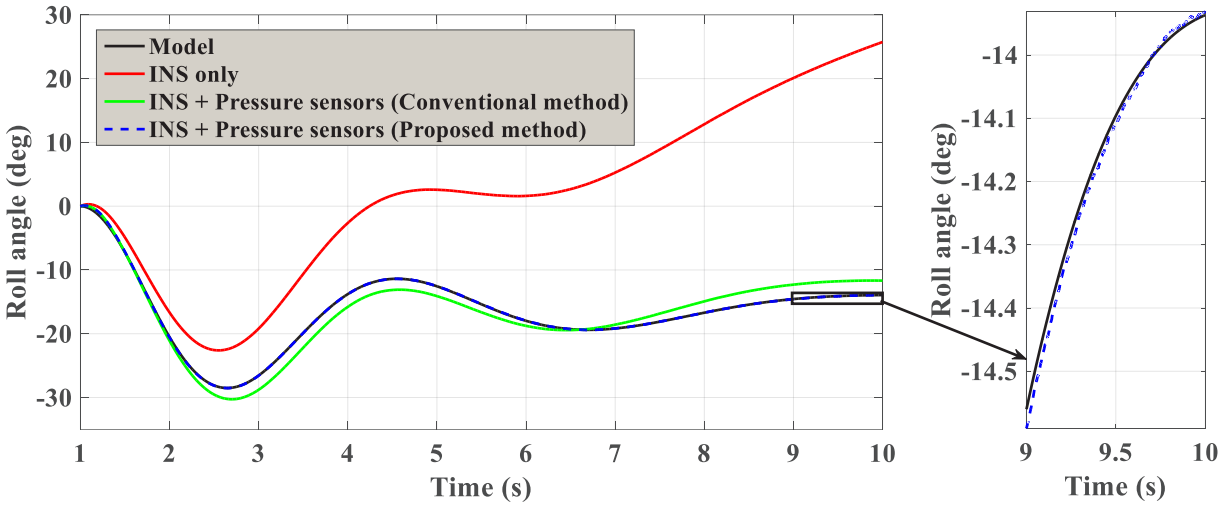

Fig. 6. Simulation results of roll angle

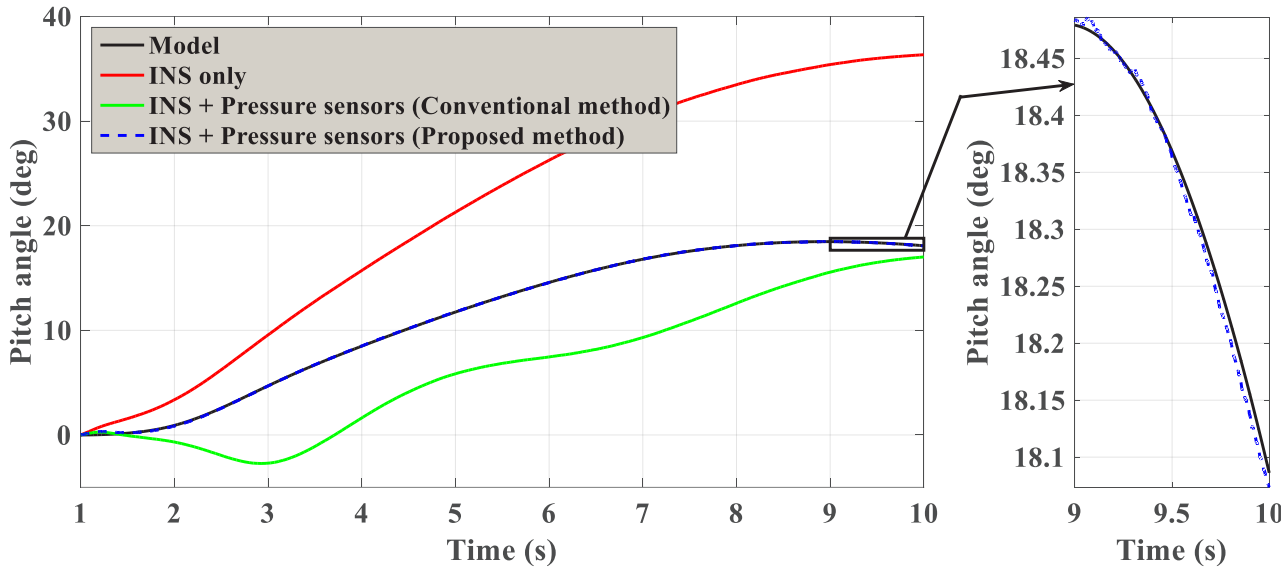

Fig. 7. Simulation results of pitch angle

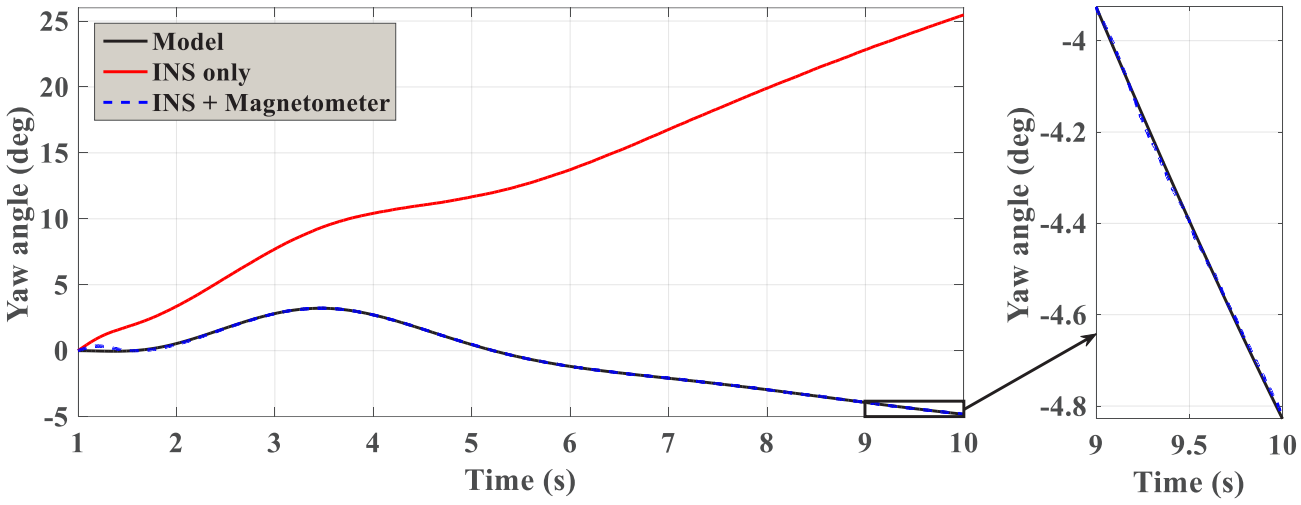

Fig. 8. Simulation results of yaw angle

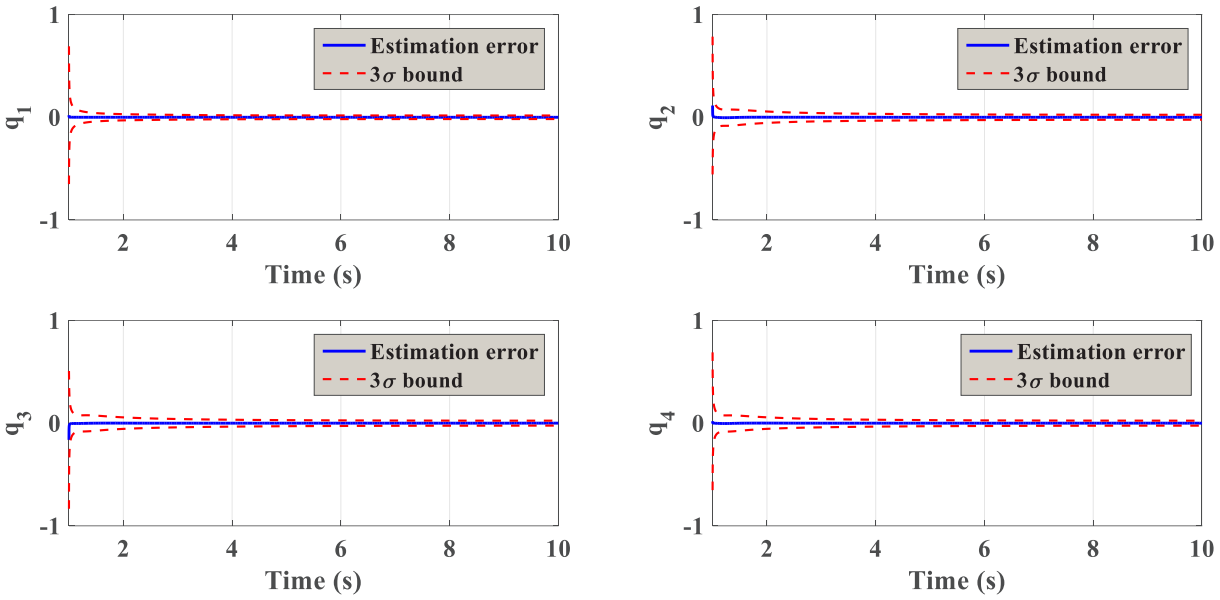

Fig. 9. The quaternions estimation error with 3σ bound

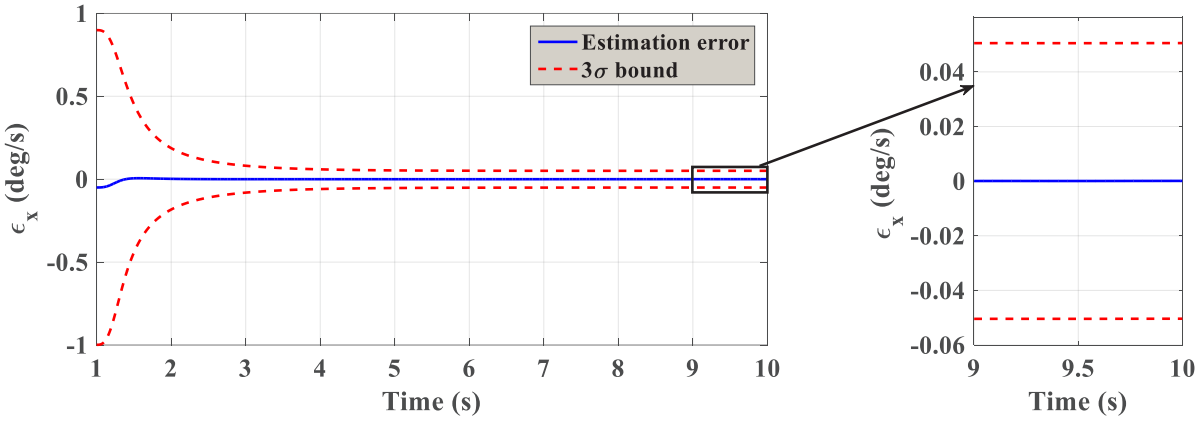

Fig. 10. Simulation results of gyroscope bias in x direction

y and z-axis are illustrated in Fig. 10 to Fig. 12. It can be seen from the results which the value of estimation errors and 3σ bounds have been converged. Also, there is no noise in gyroscope bias estimation, because the modeling of gyroscope bias is constant during the time and the uncertainty of gyroscope measurement simulation is low.

A Monte-Carlo simulation is applied for 200 consecutive runs and the RMS error of estimation is gathered in Table 1. According to Table 1, by using conventional static pressure approach the estimated RMSE of roll angle is much less than the measured RMSE by INS. But, the estimated RMSE of roll angle by proposed approach is converged to zero. Also, The RMSE of pitch angle which only measures by INS is more than the estimated RMSE of conventional approach and the estimated RMSE of pitch angle using proposed approach is converged to zero. The RMSE of yaw angle which measures by INS is more than conventional approach and the RMSE of conventional approach is more than the RMSE of proposed approach. As referred, we used quaternion method for UUV navigation. Then, the KF uses quaternion observation and we must convert the orientation observation to quaternion observation. Accordingly, in the conventional approach, tilt observation effect on the yaw angle observation and the estimation error increases.

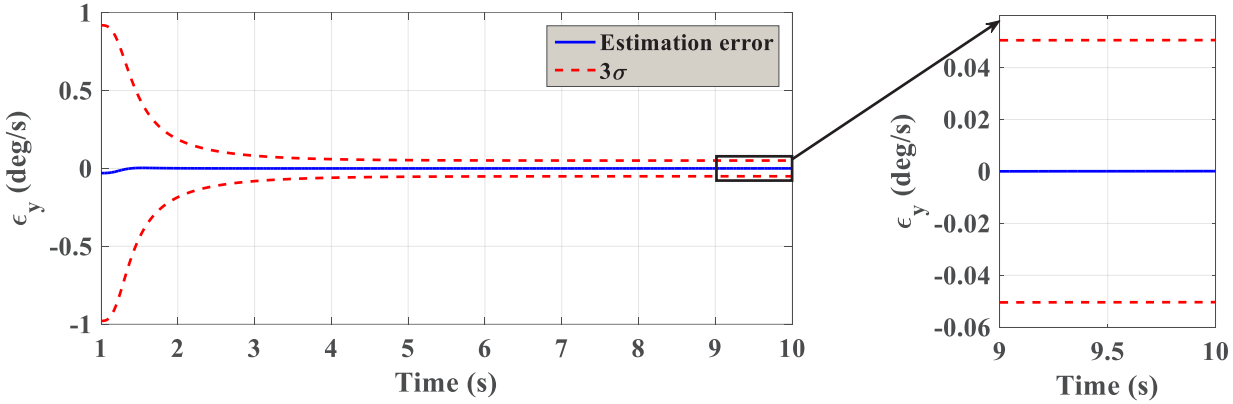

Fig. 11. Simulation results of gyroscope bias in y direction

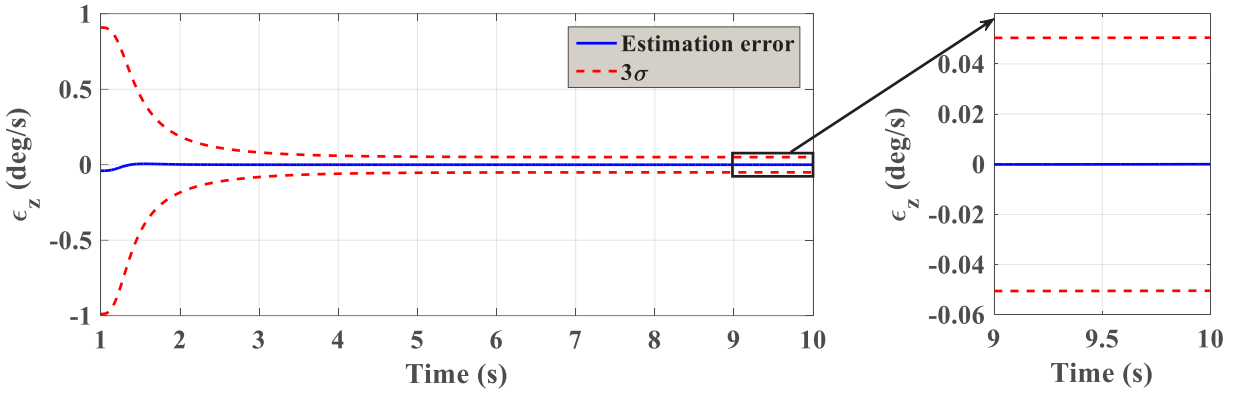

Fig. 12. Simulation results of gyroscope bias in z direction

Table 1. RMSE of 200 runs Monte-Carlo simulation

State (unit)	RMSE		
	INS only	Conventional approach	Proposed approach
Roll angle (deg)	21.6847	1.6223	0.0808
Pitch angle (deg)	11.4442	5.6186	0.0503
Yaw angle (deg)	16.5894	1.1129	0.0636
Gyroscope bias in x direction (deg/s)	-----	0.0119	0.0072
Gyroscope bias in y direction (deg/s)	-----	0.0303	0.0043
Gyroscope bias in z direction (deg/s)	-----	0.0072	0.0058

7- Conclusion

This paper deals with estimation of tilt based on pressure sensors for UUV navigation. The proposed approach considers the relation between the static and the dynamic pressure caused by the sea waves and the tilt angle as the measurement model. This causes high accuracy in pressure sensor simulation especially when the dynamic of environment increases. Tilt was estimated using pressure measurements and EKF. These estimations with magnetometer and GNSS data were used as measurements in an UUV navigation simulation loop and orientation and gyroscope bias was estimated. Tilt simulation results show that the proposed approach is effective to estimate tilt. However, conventional approach had error and INS measurements diverged from the model values. Also, the simulation results of gyroscope bias were satisfied and the estimations error value was converged. Moreover, a Monte-Carlo simulation developed based on the 200 consecutive runs and the RMSE of the estimations presented. The tilt estimation using conventional approach had RMSE but, using proposed approach the RMSE converged to zero. Although, we used GNSS to measure velocity measurements, but the velocity of UUV can be estimated using pressure sensors and this is proposed for related future research.

References

[1] D. Titterton, J.L. Weston, J. Weston, Strapdown inertial navigation technology, IET, 2004.

[2] C. Chao, Z. Jiankang, J. Hu, Improving robustness of the MAV yaw angle estimation for low-cost INS/GPS integration aided with tri-axial magnetometer calibrated by rotating the ellipsoid model, IET Radar, Sonar & Navigation, 14(1) (2020) 61-70.

[3] N.Y. Ko, H.T. Choi, C.-M. Lee, Y.S. Moon, Attitude estimation using depth measurement and AHRS data for underwater vehicle navigation, in: OCEANS 2016-Shanghai, IEEE, 2016, pp. 1-4.

[4] A. Baruch, Y. Mazal, B. Braginsky, H. Guterman, Attitude estimation of AUVs based on a network of pressure sensors, IEEE Sensors Journal, 20(14) (2020) 7988-7996.

[5] S. Zhigang, M. Xiaochuan, L. Yu, Y. Shefeng, Attitude determination of autonomous underwater vehicles based on pressure sensor array, in: 2015 34th Chinese Control Conference (CCC), IEEE, 2015, pp. 5517-5520.

[6] G. Liu, M. Wang, L. Xu, A. Incecik, M.A. Sotelo, Z. Li, W. Li, A new bionic lateral line system applied to pitch motion parameters perception for autonomous underwater vehicles, Applied Ocean Research, 99 (2020) 102142.

[7] G. Vitale, A. D'Alessandro, A. Costanza, A. Fagiolini, Low-cost underwater navigation systems by multi-pressure measurements and AHRS data, in: OCEANS 2017-Aberdeen, IEEE, 2017, pp. 1-5.

[8] H. Nourmohammadi, J. Keighobadi, Decentralized INS/GNSS system with MEMS-grade inertial sensors using QR-factorized CKF, IEEE Sensors Journal, 17(11) (2017) 3278-3287.

[9] T.T.J. Prestero, Verification of a six-degree of freedom simulation model for the REMUS autonomous underwater vehicle, Massachusetts institute of technology, 2001.

[10] I.B. Saksvik, A. Alcocer, V. Hassani, A deep learning approach to dead-reckoning navigation for autonomous underwater vehicles with limited sensor payloads, in: OCEANS 2021: San Diego–Porto, IEEE, 2021, pp. 1-9.

[11] F.M. Yaul, A flexible underwater pressure sensor array for artificial lateral line applications, Massachusetts Institute of Technology, 2011.

[12] H. Nourmohammadi, J. Keighobadi, Integration scheme for SINS/GPS system based on vertical channel decomposition and in-motion alignment, AUT Journal of Modeling and Simulation, 50(1) (2018) 13-22.

[13] Z. Huang, Z. Su, B. Huang, S. Song, J. Li, Quaternion-based finite-time fault-tolerant trajectory tracking control for autonomous underwater vehicle without unwinding, ISA transactions, 131 (2022) 15-30.

[14] X. Mu, B. He, S. Wu, X. Zhang, Y. Song, T. Yan, A practical INS/GPS/DVL/PS integrated navigation algorithm and its application on Autonomous Underwater Vehicle, Applied Ocean Research, 106 (2021) 102441.

HOW TO CITE THIS ARTICLE

M. Amuei, S. M. Dehghan, H. Nourmohammadi, M. AlirezaPouri, Tilt estimation using pressure sensors for unmanned underwater vehicle navigation, AUT J. Model. Simul., 54(2) (2022) 161-172.

DOI: 10.22060/miscj.2022.21580.5290